



Distributed fixed-time consensus-based formation tracking for multiple nonholonomic wheeled mobile robots under directed topology

Xianghang Zhang, Zhaoxia Peng, Shichun Yang, Guoguang Wen & Ahmed Rahmani

To cite this article: Xianghang Zhang, Zhaoxia Peng, Shichun Yang, Guoguang Wen & Ahmed Rahmani (2019): Distributed fixed-time consensus-based formation tracking for multiple nonholonomic wheeled mobile robots under directed topology, International Journal of Control, DOI: [10.1080/00207179.2019.1590646](https://doi.org/10.1080/00207179.2019.1590646)

To link to this article: <https://doi.org/10.1080/00207179.2019.1590646>



Accepted author version posted online: 05 Mar 2019.
Published online: 21 Mar 2019.



Submit your article to this journal [↗](#)




Article views: 17



View Crossmark data [↗](#)



Distributed fixed-time consensus-based formation tracking for multiple nonholonomic wheeled mobile robots under directed topology

Xianghang Zhang^a, Zhaoxia Peng^{a,b,c}, Shichun Yang^{a,b}, Guoguang Wen^d  and Ahmed Rahmani^e

^aSchool of Transportation Science and Engineering, Beihang University, Beijing, People's Republic of China; ^bBeijing Engineering Center for Clean Energy & High Efficient Power, Beihang University, Beijing, People's Republic of China; ^cLaboratoire international associé, Beihang University, Beijing, People's Republic of China; ^dDepartment of Mathematics, Beijing Jiaotong University, Beijing, People's Republic of China; ^eCRISTAL, UMR CNRS 9189, Ecole Centrale de Lille, Villeneuve d'Ascq, France

ABSTRACT

This paper investigates the distributed fixed-time consensus-based formation tracking problems for multiple nonholonomic wheeled mobile robots under a directed interaction topology. The distributed fixed-time consensus-based controllers under the directed interaction topology are proposed for the multiple wheeled mobile robots with nonholonomic constraints, which can guarantee the group of robots converge to a predefined formation pattern with its centroid moving along the predefined reference trajectory in a fixed time. The fixed-time formation tracking can be achieved within a fixed settling time, which is independent of the initial states of the whole system. Moreover, the conditions of formation stability control are analysed by utilising graph and Lyapunov stability theories. Finally, the feasibility of the proposed distributed controllers is verified by numerical simulation.

ARTICLE HISTORY

Received 22 June 2018
Accepted 27 February 2019

KEYWORDS

Nonholonomic wheeled mobile robots; formation control; fixed-time; consensus-based; directed topology; Lyapunov stability

1. Introduction

Over the past few years, the issue of cooperative control of multiple nonholonomic wheeled mobile robots has received considerable attention. The formation control of multi-robot system can accomplish a complex task like exploration, surveillance and security, search and rescue operations, and cooperative transport, which can not be completed by a single robot (Cheng, Wang, Ren, Hou, & Tan, 2016; Dong, Yu, Shi, & Zhong, 2015; Sarkar & Kar, 2016; Wang, Wu, Huang, Ren, & Wu, 2017). There are a number of strategies to maintain the multi-robot formation shape, including leader–follower (Das et al., 2002; Peng, Wen, Rahmani, & Yu, 2013; Shojaei, 2017), behaviour-based (Balch & Arkin, 1998; Lawton, Beard, & Young, 2003), and virtual structure (Hu, 2001; Lewis & Tan, 1997). Since the leader–follower is very easy to understand mathematically and shows good scalability, it is extensively applied.

In the literature (Chu, Peng, Wen, & Rahmani, 2017; Peng, Wen, Yang, & Rahmani, 2016), many consensus-based control strategies have been applied to achieve the formation tracking control of multi-robot system. For the consensus-based formation tracking control of multi-robot system, convergence speed is an important performance indicator. But most of previous studies only consider the asymptotic consensus, which means that convergence is achieved when time goes to infinity. Olfati-Saber and Murray (2004) introduced a typical protocol, which was shown that the convergence speed depends on the algebraic connectivity. Olfati-Saber (2005) presented some approaches on improving the algebraic connectivity, but it is still shown to converge asymptotically. In order to enhance the speed of

convergence, the finite-time control technique has been introduced to make the states of the system achieve high-speed convergence (Du, Jiang, Wen, Zhu, & Cheng, 2018; Du, Zhu, Wen, Duan, & Lü, 2019; Xiao, Hu, & Zhang, 2015). In Wen, Yu, Peng, and Rahmani (2016), a distributed finite-time control law was proposed by using finite-time consensus approach to solve the consensus tracking problem for nonlinear multi-agent systems. Zhao, Duan, and Wen (2014) investigated the distributed finite-time consensus problem of double integrators without velocity measurements. The consensus problem of multi-robot system in the form of high-order chained structure was considered in Du, Wen, Cheng, He, and Jia (2017), Du, Wen, Yu, Li, and Chen (2015), and a finite-time cooperative controller was proposed which ensures that the states consensus is attained in a finite time.

However, those above literatures considered that all the setting times depend on the initial states of the system. Unfortunately, information about initial states can be inaccurate or even unavailable in an unknown environment. Therefore, it does not make much sense if the initial states are very large or unavailable. In this situation, fixed-time stability theory has been introduced to make the setting time regardless of the initial conditions (Ni, Liu, Liu, & Hu, 2017; Polyakov, 2012), which has been applied to the multi-agent systems. In Zhang and Jia (2015), fixed-time consensus laws were proposed for multi-agent systems with linear and nonlinear state measurements. In addition, (Hong, Yu, Wen, & Yu, 2016) proposed two fixed-time control laws to solve the leaderless and leader–follower consensus problems for multi-agent systems with uncertain

disturbances. Chu, Peng, Wen, and Rahmani (2018) investigated the robust fixed-time consensus tracking problem of second-order multi-agent systems under undirected topology, in which the designed fixed-time controllers can be applied to deal with a simplified nonholonomic multi-robot systems. However, the angular velocity of robot was not considered in the control protocols.

To the author's knowledge, few results about fixed-time control for multi-robots systems with nonholonomic constraints are available till now. Motivated by the aforementioned discussions, in this paper the distributed fixed-time consensus-based formation tracking problems for multiple wheeled mobile robots under the directed interaction topology are investigated. There are two main contributions. Firstly, the distributed fixed-time consensus-based formation tracking controllers under directed interaction topology are proposed for the multiple wheeled mobile robots with nonholonomic constraints. Second, the fixed-time formation tracking can be achieved within a fixed settling time, and the fixed setting time of the multi-robots systems is independent of the robots' initial states, which can be obtained by the predefined parameters, the weighted adjacency matrix and the number of the wheeled mobile robots.

Compared with existing works in the literature, the main contributions and advantages of this paper are summarised as follows: Firstly, in contrast to the existing works on fixed-time cooperative control (Chu et al., 2018; Hong et al., 2016; Zhang & Jia, 2015) for multi-agent system, in which the agent system always were considered to be linear system. In this paper, the wheeled mobile robot is a nonholonomic and nonlinear constrained system. Secondly, many existing works for formation tracking problem of multi-robots system under undirected communication topologies were studied (Peng et al., 2016; Wenjie, 2011; Wen et al., 2016). However, in practice bilateral communication between robots is not unusual. In this paper the information communication topology is considered as to be directed, which can reduce information exchange among robots, improve the fault tolerance and reduce energy consumption of system. Thirdly, the proposed controllers are distributed, which means that each robot can only obtain information from its neighbours. The robustness of the group of wheeled mobile robots has also been improved.

The remainder of this paper is organised as follows. Section 2 introduces the preliminaries and the problem formulation. The distributed fixed-time formation tracking control algorithm is presented in Section 3. Section 4 verifies the theoretical analysis through simulations results. Finally, some conclusions are given in Section 5.

2. Preliminaries and problem formulation

2.1 Notations

Throughout this paper, $\mathbf{1}_m = [1, 1, \dots, 1]^T \in \mathbb{R}^m$, and $\mathbf{0}_m = [0, 0, \dots, 0]^T \in \mathbb{R}^m$ ($\mathbf{0}$ for short, when there is no confusion). For convenience, in the sequel, set $\text{sig}(x_j)^\alpha = |x_j|^\alpha \text{sign}(x_j)$, $\alpha > 0$, where $\text{sign}(x_j) \triangleq x_j/|x_j|$ for $x_j \neq 0$, and $\text{sign}(0) = 0$. For any $x = (x_1, x_2, \dots, x_m)^T \in \mathbb{R}^m$, denote $|x| = [|x_1|, |x_2|, \dots, |x_m|]^T$, $\text{diag}(x) = \text{diag}\{x_1, x_2, \dots, x_m\}$, $\text{sig}(x)^\alpha = [\text{sig}(x_1)^\alpha, \text{sig}(x_2)^\alpha, \dots, \text{sig}(x_m)^\alpha]^T$ and $\text{sign}(x) = [\text{sign}(x_1), \text{sign}(x_2), \dots, \text{sign}(x_m)]^T$.

$(x_2)^\alpha, \dots, \text{sig}(x_m)^\alpha]^T$ and $\text{sign}(x) = [\text{sign}(x_1), \text{sign}(x_2), \dots, \text{sign}(x_m)]^T$.

2.2 Preliminaries

In this paper, the system model and the information exchange communication topology of the robots are established by directed graph. A multi-robot system can be described by a directed graph $\mathcal{G} = (\mathcal{V}, \mathcal{E}, \mathcal{A})$, where $\mathcal{V} = \{v_1, \dots, v_m\}$ is the set of nodes, $\mathcal{E} \subseteq \mathcal{V} \times \mathcal{V}$ represents the set of edges, and $\mathcal{A} = [a_{ij}]_{m \times m}$ is a weighted adjacency matrix. Here, each node v_i in \mathcal{V} corresponds to a robot i , and each edge $(v_i, v_j) \in \mathcal{E}$ describes that the robot i is a neighbour of robot j , and the robot j has access to the state information of the robot i . The weighted adjacency matrix $\mathcal{A} = [a_{ij}]_{m \times m}$ of a directed graph \mathcal{G} is given by

$$a_{ij} = \begin{cases} 1, & \text{for } (v_j, v_i) \in \mathcal{E}, \\ 0, & \text{otherwise.} \end{cases}$$

In this paper, let $a_{jj} = 0$, that is means that self-edges are not existed. The neighbour set of node j is given by $\mathcal{N}_j = \{v_i \in \mathcal{V} : a_{ji} \neq 0\} = \{v_i \in \mathcal{V} : (j, i) \in \mathcal{E}\}$. The Laplacian matrix \mathcal{L} of a directed graph \mathcal{G} is introduced as $\mathcal{L} = \mathcal{D} - \mathcal{A}$, where $\mathcal{D} = \text{diag}\{d_1, d_2, \dots, d_m\}$, and $d_j = \sum_{i=1, i \neq j}^m a_{ji}$, $j \in \{1, \dots, m\}$.

Let $\mathcal{B} = \text{diag}\{b_1, b_2, \dots, b_m\}$, and b_j denote the connection weight between robot j ($1 \leq j \leq m$) and the virtual leader 0. If robot j has access the state information of the virtual leader 0, then $b_j > 0$, otherwise $b_j = 0$.

In order to develop our main results, the following lemmas shall be introduced.

Lemma 2.1 (Hu & Feng, 2010): Define $\mathcal{M} = \mathcal{L} + \mathcal{B}$, then the matrix \mathcal{M} is a positive stable matrix whose eigenvalues have positive real parts if the graph \mathcal{G} has a directed spanning tree.

Lemma 2.2 (Polyakov, 2012): Consider the system as follows

$$\dot{x}(t) = f(x, t), \quad (1)$$

where $x \in \mathbb{R}^N$ and $f(x, t) : \mathbb{R}^N \times \mathbb{R}_+ \rightarrow \mathbb{R}^N$ is a nonlinear function. Suppose that the equilibrium point of (1) contains the origin. If there exists a continuous radially unbounded function $V(x) : \mathbb{R}^N \rightarrow \mathbb{R}_+ \cup \{0\}$ such that $V(x) = 0 \Leftrightarrow x = 0$ and satisfies the inequality

$$D^*V(x(t)) \leq -\alpha V^p(x(t)) - \beta V^q(x(t)),$$

for $\alpha > 0, \beta > 0, 0 < p < 1, q > 1$. Then the origin is the global fixed-time stable equilibrium point of (1) and the setting time is bounded with

$$T_{\max} = \frac{1}{\alpha(1-p)} + \frac{1}{\beta(q-1)}.$$

Lemma 2.3 (Zuo & Tie, 2016): If $y_1, y_2, \dots, y_n \geq 0$, then

$$\sum_{i=1}^n y_i^p \geq \left(\sum_{i=1}^n y_i \right)^p, \quad 0 < p \leq 1,$$

$$\sum_{i=1}^n y_i^p \geq n^{1-p} \left(\sum_{i=1}^n y_i \right)^p, \quad 1 < p \leq \infty.$$

2.3 Problem formulation

A multi-robot system composed of m nonholonomic wheeled mobile robots is considered. Suppose that all nonholonomic wheeled mobile robots are the same (see Figure 1). The kinematics of the wheeled mobile robot j can be described by

$$\begin{aligned}\dot{x}_j(t) &= v_j(t) \cos \theta_j(t), \\ \dot{y}_j(t) &= v_j(t) \sin \theta_j(t), \\ \dot{\theta}_j(t) &= \omega_j(t).\end{aligned}\quad (2)$$

where x_j, y_j, θ_j denote the coordinate and orientation of the wheeled mobile robot j , respectively. v_j and ω_j denote the linear and angular velocity of the wheeled mobile robot j , respectively.

Our control object of this paper is to design the appropriate control inputs $v_j(t)$ and $\omega_j(t)$ for the nonholonomic wheeled mobile robot j to make m wheeled mobile robots form a predefined formation pattern \mathcal{F} and track a specified reference trajectory (virtual leader's trajectory) simultaneously in a fixed-time T .

Utilizing orthogonal coordinates (p_{jx}, p_{jy}) to define the desired formation pattern \mathcal{F} . (p_{0x}, p_{0y}) is the orthogonal coordinate of the virtual leader. For simplicity, we assume that $p_{0x} = 0, p_{0y} = 0$. Here, the kinematics of the virtual leader is also specified by

$$\dot{x}_0(t) = v_0(t) \cos \theta_0(t), \quad (3)$$

$$\dot{y}_0(t) = v_0(t) \sin \theta_0(t), \quad (4)$$

$$\dot{\theta}_0(t) = \omega_0(t). \quad (5)$$

Definition 2.4: For any given bounded initial states, if there exists a fixed-time T , it has

$$\lim_{t \rightarrow T} \begin{bmatrix} x_j(t) - x_i(t) \\ y_j(t) - y_i(t) \end{bmatrix} = \begin{bmatrix} p_{jx} - p_{ix} \\ p_{jy} - p_{iy} \end{bmatrix}, \quad (6)$$

$$\lim_{t \rightarrow T} (\theta_j(t) - \theta_0(t)) = 0, \quad (7)$$

$$\lim_{t \rightarrow T} \left(\sum_{j=1}^m \frac{x_j(t)}{m} - x_0(t) \right) = 0,$$

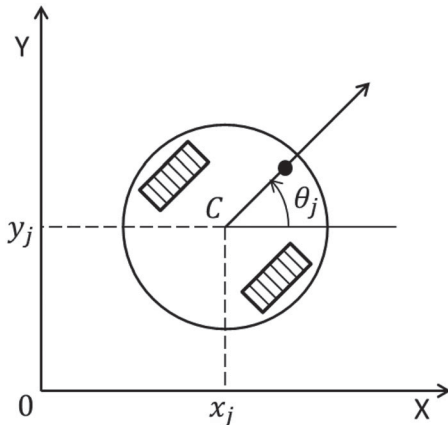


Figure 1. Model of wheeled mobile robot.

$$\lim_{t \rightarrow T} \left(\sum_{j=1}^m \frac{y_j(t)}{m} - y_0(t) \right) = 0. \quad (8)$$

for $1 \leq j \leq m$, then the desired formation tracking is accomplished in fixed time T by the multi-robot system.

The following assumptions are given to realised our control objective.

Assumption 2.5: The orientation θ_j of the wheeled mobile robot j ($0 \leq j \leq m$) is bounded, and the angular velocity ω_j of the wheeled mobile robot j ($0 \leq j \leq m$) is also bounded. And, $|\omega_j| \leq \kappa$, where κ is a positive constant.

Assumption 2.6: The state of the virtual leader is available to only a subset of followers, and the subset is not null.

Assumption 2.7: The communication directed graph \mathcal{G} has a directed spanning tree with the root node being that of the leader.

3. Main result

3.1 Transformation and control objective

Since the wheeled mobile robot system is nonholonomic, it is much more complicated than a linear system. So we need to linearise the robot system partially. A transformation is given by Murray and Sastry (1993) as follows

$$\begin{aligned}z_{1j} &= \theta_j, \\ z_{2j} &= (x_j - p_{jx}) \sin \theta_j - (y_j - p_{jy}) \cos \theta_j, \\ z_{3j} &= (x_j - p_{jx}) \cos \theta_j + (y_j - p_{jy}) \sin \theta_j, \\ u_{1j} &= \omega_j, \\ u_{2j} &= v_j - u_{1j} z_{2j},\end{aligned}\quad (9)$$

with the inputs u_{1j} and u_{2j} , where $0 \leq j \leq m$. Then, the formation tracking control problem for multi-robot system can be converted into a state consensus problem. By converting, the wheeled robot system (2) can be rewritten as

$$\dot{z}_{1j} = u_{1j}, \quad (10)$$

$$\dot{z}_{2j} = u_{1j} z_{3j}, \quad (11)$$

$$\dot{z}_{3j} = u_{2j}. \quad (12)$$

From the transformation(9) and the original control objectives (6)–(8), we can get the new control objectives as follows

$$\lim_{t \rightarrow T} (z_{1j} - z_{10}) = 0 \quad (13)$$

$$\lim_{t \rightarrow T} (z_{2j} - z_{20}) = 0, \quad (14)$$

$$\lim_{t \rightarrow T} (z_{3j} - z_{30}) = 0. \quad (15)$$

for $0 \leq j \leq m$.

Remark 1: Due to the nonlinear characteristics of nonholonomic system. Traditional linear control theory(including traditional consensus control strategy) is difficult to directly used

to the formation control for nonholonomic mobile robots system. In order to tackle the nonholonomic constraints in (3)–(5), in this paper, the authors use a classical variable transformations (9) (Murray & Sastry, 1993) to linearise the nonholonomic robot system to a linear-like chained system (8)–(10). Hence, the formation control problem is converted as the consensus problem of the new variables, and the distributed control design and the stability analysis can be handled.

Lemma 3.1: *If the new control objectives (13)–(14) are achieved for $0 \leq j \leq m$, then the original control objectives (6)–(8) can be satisfied in fixed time T , that is to say, the desired formation pattern \mathcal{F} of m mobile robots are formed in fixed time T .*

Proof: Based on the input and state transformation (9), we can get that

$$\begin{aligned} \theta_j &= z_{1j}, \\ \begin{bmatrix} x_j - p_{jx} \\ y_j - p_{jy} \end{bmatrix} &= \begin{bmatrix} \sin \theta_j & \cos \theta_j \\ -\cos \theta_j & \sin \theta_j \end{bmatrix} \times \begin{bmatrix} z_{2j} \\ z_{3j} \end{bmatrix}. \end{aligned}$$

If (13)–(14) are satisfied, it has follows

$$\begin{aligned} \lim_{t \rightarrow T} \begin{bmatrix} x_j - p_{jx} \\ y_j - p_{jy} \end{bmatrix} &= \lim_{t \rightarrow T} \begin{bmatrix} \sin \theta_j & \cos \theta_j \\ -\cos \theta_j & \sin \theta_j \end{bmatrix} \times \begin{bmatrix} z_{2j} \\ z_{3j} \end{bmatrix} \\ &= \begin{bmatrix} \sin \theta_0 & \cos \theta_0 \\ -\cos \theta_0 & \sin \theta_0 \end{bmatrix} \begin{bmatrix} z_{20} \\ z_{30} \end{bmatrix} \\ &= \begin{bmatrix} x_0 \\ y_0 \end{bmatrix}, \\ \lim_{t \rightarrow T} \theta_j &= \theta_0. \end{aligned}$$

Then, it can be easily obtained that the control objectives (6)–(8) are held. This proof is completed. ■

Remark 2: Based on the transformation (9), if the new control objectives (13)–(15) for the new systems (10)–(12) are achieved, that is to say, the the control objectives (6)–(8) are achieved for the system (2). Thus, in the next subsection, we will design the distributed fixed-time consensus-based control protocols under directed topology for the new systems for the systems (10)–(12).

3.2 Distributed fixed-time control algorithm under directed topology

In order to analyse the leader-following consensus problem for the dynamic system (10)–(12), the tracking errors between the robot j and the leader are defined as

$$\begin{aligned} \tilde{z}_{1j} &= z_{1j} - z_{10}, \\ \tilde{z}_{2j} &= z_{2j} - z_{20}, \\ \tilde{z}_{3j} &= z_{3j} - z_{30}. \end{aligned} \quad (16)$$

Define the local relative tracking errors of the robot j ($1 \leq j \leq m$) as

$$e_{1j} = \sum_{i \in N_j} a_{ji}(z_{1j} - z_{1i}) + b_j(z_{1j} - z_{10}), \quad (17)$$

$$e_{2j} = \sum_{i \in N_j} a_{ji}(z_{2j} - z_{2i}) + b_j(z_{2j} - z_{20}), \quad (18)$$

$$e_{3j} = \sum_{i \in N_j} a_{ji}(z_{3j} - z_{3i}) + b_j(z_{3j} - z_{30}). \quad (19)$$

Let $z_1 = [z_{11}, \dots, z_{1m}]^T$, $z_2 = [z_{21}, \dots, z_{2m}]^T$, $z_3 = [z_{31}, \dots, z_{3m}]^T$, $\tilde{z}_1 = [\tilde{z}_{11}, \dots, \tilde{z}_{1m}]^T$, $\tilde{z}_2 = [\tilde{z}_{21}, \dots, \tilde{z}_{2m}]^T$, $\tilde{z}_3 = [\tilde{z}_{31}, \dots, \tilde{z}_{3m}]^T$, $e_1 = [e_{11}, \dots, e_{1m}]^T$, $e_2 = [e_{21}, \dots, e_{2m}]^T$, $e_3 = [e_{31}, \dots, e_{3m}]^T$, then (17)–(19) can be written into vectors form as follows

$$e_1 = \mathcal{M}\tilde{z}_1, \quad (20)$$

$$e_2 = \mathcal{M}\tilde{z}_2, \quad (21)$$

$$e_3 = \mathcal{M}\tilde{z}_3. \quad (22)$$

For convenience of calculation, the auxiliary local relative tracking error is defined as follows

$$\bar{e}_2 = e_2 - \mathcal{M} \text{diag}(z_3) \tilde{z}_1, \quad (23)$$

where $\bar{e}_2 = [\bar{e}_{21}, \dots, \bar{e}_{2m}]^T$.

Remark 3: Note from (20) that if $e_1(t) \rightarrow \mathbf{0}$, then $\tilde{z}_1 \rightarrow \mathbf{0}$. From (22) and (16), if $e_3(t) \rightarrow \mathbf{0}$, then one has $z_3 \rightarrow \mathbf{1}_m z_{30}$. Furthermore, according to Equation (23), if the condition $\bar{e}_2(t) \rightarrow \mathbf{0}$ is also held, then it can be easily obtained that $e_2(t) \rightarrow \mathbf{0}$. Consequently, if $e_1(t) \rightarrow \mathbf{0}$, $\bar{e}_2(t) \rightarrow \mathbf{0}$ and $e_3(t) \rightarrow \mathbf{0}$, then $e_2(t) \rightarrow \mathbf{0}$. Hence, in the following section we will prove $e_1(t) \rightarrow \mathbf{0}$, $\bar{e}_2(t) \rightarrow \mathbf{0}$ and $e_3(t) \rightarrow \mathbf{0}$ in fixed time.

According to the tracking errors (16) and the dynamic system (10)–(12), the dynamic system of tracking errors can be derived as follows

$$\dot{\tilde{z}}_{1j} = u_{1j} - u_{10}, \quad (24)$$

$$\dot{\tilde{z}}_{2j} = u_{1j}z_{3j} - u_{10}z_{30} = u_{10}\tilde{z}_{3j} + z_{3j}(u_{1j} - u_{10}), \quad (25)$$

$$\dot{\tilde{z}}_{3j} = u_{2j} - u_{20}. \quad (26)$$

Equations (24)–(26) can be written into the vector form as

$$\dot{\tilde{z}}_1 = u_1 - \mathbf{1}_m u_{10}, \quad (27)$$

$$\dot{\tilde{z}}_2 = u_{10}\tilde{z}_3 + \text{diag}(z_3)(u_1 - \mathbf{1}_m u_{10}), \quad (28)$$

$$\dot{\tilde{z}}_3 = u_2 - \mathbf{1}_m u_{20}, \quad (29)$$

where $u_1 = [u_{11}, u_{12}, \dots, u_{1m}]^T$, $u_2 = [u_{21}, u_{22}, \dots, u_{2m}]^T$. According to the local relative tracking errors (20)–(22) and the tracking errors (27)–(29), the local relative tracking errors of the system can be derived as follows

$$\dot{e}_1 = \mathcal{M}u_1 - \mathcal{B}\mathbf{1}_m u_{10}, \quad (30)$$

$$\dot{e}_2 = u_{10}e_3 + \mathcal{M} \text{diag}(z_3)(u_1 - \mathbf{1}_m u_{10}), \quad (31)$$

$$\dot{e}_3 = \mathcal{M}u_2 - \mathcal{B}\mathbf{1}_m u_{20}. \quad (32)$$

Then, the local relative tracking error (23) can be derived as

$$\dot{\bar{e}}_2 = \dot{e}_2 - \mathcal{M} \text{diag}(z_3) \dot{\tilde{z}}_1 - \mathcal{M} \text{diag}(\dot{z}_3) \tilde{z}_1. \quad (33)$$

Substituting (12), (27) and (31) into (33), we get

$$\dot{\bar{e}}_2 = u_{10}e_3 - \mathcal{M}diag(u_2)\bar{z}_1. \quad (34)$$

In order to guarantee the fixed-time formation tracking, we propose the following control inputs for the wheeled mobile robot j ($1 \leq j \leq m$) as

$$u_{1j} = \frac{1}{\sum_{i \in \mathcal{N}_j} a_{ji} + b_j} (-k_1 sig(e_{1j})^\alpha - k_3 sig(e_{1j})^\beta + b_j u_{10} + \sum_{i \in \mathcal{N}_j} a_{ji} u_{1i} + u_{1j}^*), \quad (35)$$

$$u_{2j} = \frac{1}{\sum_{i \in \mathcal{N}_j} a_{ji} + b_j} (-k_1 sig(e_{3j})^\alpha - k_3 sig(e_{3j})^\beta + b_j u_{20} + \sum_{i \in \mathcal{N}_j} a_{ji} u_{2i} - k_2 sign(e_{3j})|\bar{e}_{2j}|), \quad (36)$$

with

$$u_{1j}^* = \frac{1}{\sum_{i \in \mathcal{N}_j} a_{ij} + b_j} \left(u_{2j} \left(\sum_{i \in \mathcal{N}_j} a_{ij} (\bar{e}_{2j} - \bar{e}_{2i}) + b_j \bar{e}_{2j} \right) + \sum_{i \in \mathcal{N}_j} a_{ij} u_{1i}^* \right), \quad (37)$$

where k_1, k_2, k_3, α and β are positive constants, satisfying $k_2 > \kappa$, $0 < \alpha < 1$ and $\beta > 1$. According to control input (35), we can get

$$\left(\sum_{i \in \mathcal{N}_j} a_{ji} + b_j \right) u_{1j} = -k_1 sig(e_{1j})^\alpha - k_3 sig(e_{1j})^\beta + b_j u_{10} + \sum_{i \in \mathcal{N}_j} a_{ji} u_{1i} + u_{1j}^*. \quad (38)$$

Equation (38) can be rewritten as

$$\sum_{i \in \mathcal{N}_j} a_{ji} (u_{1j} - u_{1i}) + b_j u_{1j} = -k_1 sig(e_{1j})^\alpha - k_3 sig(e_{1j})^\beta + b_j u_{10} + u_{1j}^*. \quad (39)$$

Equation (39) can be written in vector form as

$$\mathcal{M}u_1 = -k_1 sig(e_1)^\alpha - k_3 sig(e_1)^\beta + \mathcal{B}\mathbf{1}_m u_{10} + u_1^*, \quad (40)$$

where $u_1^* = [u_{11}^*, u_{12}^*, \dots, u_{1m}^*]^T$. Both sides of the Equation (40) left multiple by the matrix \mathcal{M}^{-1} , we can obtain that

$$u_1 = \mathcal{M}^{-1} [-k_1 sig(e_1)^\alpha - k_3 sig(e_1)^\beta + \mathcal{B}\mathbf{1}_m u_{10} + u_1^*]. \quad (41)$$

Similarly, we have

$$u_2 = \mathcal{M}^{-1} [-k_1 sig(e_3)^\alpha - k_3 sig(e_3)^\beta + \mathcal{B}\mathbf{1}_m u_{20} - k_2 diag(sign(e_3))|\bar{e}_2|]. \quad (42)$$

Remark 4: From the controllers (35) and (36), we can see that the control inputs u_{1j} and u_{2j} just need the information from its neighbours. Equations (41) and (42) are equivalent vector expressions of (35)–(36), which do not mean that each robot can directly obtain the information of the leader. In fact, each follower gets the information of leader from its neighbours. Therefore, the controllers are distributed.

From (37), one has

$$\left(\sum_{i \in \mathcal{N}_j} a_{ij} + b_j \right) u_{1j}^* = u_{2j} \left(\sum_{i \in \mathcal{N}_j} a_{ij} (\bar{e}_{2j} - \bar{e}_{2i}) + b_j \bar{e}_{2j} \right) + \sum_{i \in \mathcal{N}_j} a_{ij} u_{1i}^*. \quad (43)$$

Equation (43) can be rewritten as

$$\sum_{i \in \mathcal{N}_j} a_{ij} (u_{1j}^* - u_{1i}^*) + b_j u_{1j}^* = u_{2j} \left(\sum_{i \in \mathcal{N}_j} a_{ij} (\bar{e}_{2j} - \bar{e}_{2i}) + b_j \bar{e}_{2j} \right). \quad (44)$$

Equation (44) can be written in vector form as

$$\mathcal{M}^T u_1^* = diag(u_2) \mathcal{M}^T \bar{e}_2. \quad (45)$$

Both sides of the Equation (45) left multiple by the matrix $(\mathcal{M}^T)^{-1}$, we can obtain that

$$u_1^* = (\mathcal{M}^T)^{-1} diag(u_2) \mathcal{M}^T \bar{e}_2. \quad (46)$$

Based on the above deduction, the control inputs (35)–(36) can be written in vector form as follows

$$u_1 = \mathcal{M}^{-1} [-k_1 sig(e_1)^\alpha - k_3 sig(e_1)^\beta + \mathcal{B}\mathbf{1}_m u_{10} + (\mathcal{M}^T)^{-1} diag(u_2) \mathcal{M}^T \bar{e}_2], \quad (47)$$

$$u_2 = \mathcal{M}^{-1} [-k_1 sig(e_3)^\alpha - k_3 sig(e_3)^\beta + \mathcal{B}\mathbf{1}_m u_{20} - k_2 diag(sign(e_3))|\bar{e}_2|], \quad (48)$$

where $k_1 > 0, k_2 > \kappa, k_3 > 0, 0 < \alpha < 1, \beta > 1$.

Remark 5: From Lemma 2.1, if the graph \mathcal{G} has a directed spanning tree, then the matrix \mathcal{M} is positive definite. It can be easily obtained that the inverse matrix of \mathcal{M} exists, and the inverse matrix matrix of \mathcal{M}^T also exists.

Theorem 3.2: For the system in Equations (10)–(12), if the directed communication graph \mathcal{G} has a directed spanning tree and Assumption 2.6 is satisfied, then $\lim_{t \rightarrow T} (z_{1j} - z_{10}) = 0$, $\lim_{t \rightarrow T} (z_{2j} - z_{20}) = 0$ and $\lim_{t \rightarrow T} (z_{3j} - z_{30}) = 0$ in fixed-time under distributed controllers (35) and (36), in particular, $z_{1j} = z_{10}, z_{2j} = z_{20}$ and $z_{3j} = z_{30}$ for any $t \geq T$, where

$$T = \frac{2}{k_1 c_1 (1 - \alpha)} + \frac{2}{k_3 m^{\frac{1-\beta}{2}} c_3 (\beta - 1)}. \quad (49)$$

Proof: Choose the Lyapunov function candidate as follows

$$V = \frac{1}{2} (e_1^T e_1 + \bar{e}_2^T \bar{e}_2 + e_3^T e_3), \quad (50)$$

The derivative of the Lyapunov function candidate V is

$$\dot{V} = e_1^T \dot{e}_1 + \bar{e}_2^T \dot{\bar{e}}_2 + e_3^T \dot{e}_3. \quad (51)$$

Substituting (30), (32) and (34) into (51), we get

$$\begin{aligned} \dot{V} &= e_1^T [\mathcal{M}u_1 - \mathcal{B}\mathbf{1}_m u_{10}] + \bar{e}_2^T [u_{10}e_3 - \mathcal{M}diag(u_2)\tilde{z}_1] \\ &\quad + e_3^T [\mathcal{M}u_2 - \mathcal{B}\mathbf{1}_m u_{20}]. \end{aligned} \quad (52)$$

Combining control inputs (35) and (36) of the system, one has

$$\begin{aligned} \dot{V} &= e_1^T [-k_1 sig(e_1)^\alpha - k_3 sig(e_1)^\beta \\ &\quad + (\mathcal{M}^T)^{-1} diag(u_2) \mathcal{M}^T \bar{e}_2] \\ &\quad + \bar{e}_2^T [u_{10}e_3 - \mathcal{M}diag(u_2)\tilde{z}_1] \\ &\quad + e_3^T [-k_1 sig(e_3)^\alpha - k_3 sig(e_3)^\beta \\ &\quad - k_2 diag(sign(e_3))|\bar{e}_2|] \\ &= -k_1 e_1^T sig(e_1)^\alpha - k_3 e_1^T sig(e_1)^\beta - k_1 e_3^T sig(e_3)^\alpha \\ &\quad - k_3 e_3^T sig(e_3)^\beta + u_{10} \bar{e}_2^T e_3 - k_2 |e_3|^T |\bar{e}_2| \\ &\quad + \tilde{z}_1^T diag(u_2) \mathcal{M}^T \bar{e}_2 - \bar{e}_2^T \mathcal{M}diag(u_2)\tilde{z}_1. \end{aligned} \quad (53)$$

Since $|u_{10}| < \kappa$, $k_2 > \kappa$, and $\tilde{z}_1^T diag(u_2) \mathcal{M}^T \bar{e}_2 = \bar{e}_2^T \mathcal{M}diag(u_2)\tilde{z}_1$, Equation (53) can be simplified as

$$\begin{aligned} \dot{V} &\leq -k_1 e_1^T sig(e_1)^\alpha - k_3 e_1^T sig(e_1)^\beta - k_1 e_3^T sig(e_3)^\alpha \\ &\quad - k_3 e_3^T sig(e_3)^\beta \\ &= -k_1 \sum_{j=1}^m e_{1j} sig(e_{1j})^\alpha - k_3 \sum_{j=1}^m e_{1j} sig(e_{1j})^\beta \\ &\quad - k_1 \sum_{j=1}^m e_{3j} sig(e_{3j})^\alpha - k_3 \sum_{j=1}^m e_{3j} sig(e_{3j})^\beta \\ &= -k_1 \sum_{j=1}^m |e_{1j}|^{\alpha+1} - k_3 \sum_{j=1}^m |e_{1j}|^{\beta+1} \\ &\quad - k_1 \sum_{j=1}^m |e_{3j}|^{\alpha+1} - k_3 \sum_{j=1}^m |e_{3j}|^{\beta+1} \\ &= -k_1 \sum_{j=1}^m (|e_{1j}|^2)^{\frac{\alpha+1}{2}} - k_3 \sum_{j=1}^m (|e_{1j}|^2)^{\frac{\beta+1}{2}} \\ &\quad - k_1 \sum_{j=1}^m (|e_{3j}|^2)^{\frac{\alpha+1}{2}} - k_3 \sum_{j=1}^m (|e_{3j}|^2)^{\frac{\beta+1}{2}} \end{aligned} \quad (54)$$

By Lemma 2.3, we can get

$$\begin{aligned} \dot{V} &\leq -k_1 \left(\sum_{j=1}^m |e_{1j}|^2 \right)^{\frac{\alpha+1}{2}} - k_3 m^{\frac{1-\beta}{2}} \left(\sum_{j=1}^m |e_{1j}|^2 \right)^{\frac{\beta+1}{2}} \\ &\quad - k_1 \left(\sum_{j=1}^m |e_{3j}|^2 \right)^{\frac{\alpha+1}{2}} - k_3 m^{\frac{1-\beta}{2}} \left(\sum_{j=1}^m |e_{3j}|^2 \right)^{\frac{\beta+1}{2}} \\ &= -k_1 (\|e_1\|_2^{\alpha+1} + \|e_3\|_2^{\alpha+1}) \\ &\quad - k_3 m^{\frac{1-\beta}{2}} (\|e_1\|_2^{\beta+1} + \|e_3\|_2^{\beta+1}). \end{aligned} \quad (55)$$

Define $f(e_1, e_3) = \|e_1\|_2^{\alpha+1} + \|e_3\|_2^{\alpha+1}$. Then, for any $k > 0$, we can get that $f(ke_1, ke_3) = k^{\alpha+1} f(e_1, e_3)$.

When $f(e_1, e_3) > 0$, we know $V(e_1, \bar{e}_2, e_3) > 0$ and let $k = (V(e_1, \bar{e}_2, e_3))^{-\frac{1}{2}}$. For convenience, note $k = V^{-\frac{1}{2}}$, then we get that

$$V^{-\frac{\alpha+1}{2}} f(e_1, e_3) = f(V^{-\frac{1}{2}} e_1, V^{-\frac{1}{2}} e_3) \geq c_1, \quad (56)$$

where $c_1 = \min f(V^{-\frac{1}{2}} e_1, V^{-\frac{1}{2}} e_3) > 0$. From (56), we can easily get $f(e_1, e_3) \geq c_1 V^{\frac{\alpha+1}{2}}$.

When $f(e_1, e_3) = 0$, according to Remark 7, it is easy to obtain that $\bar{e}_2 = \mathbf{0}$, that is to say, $(e_1^T, \bar{e}_2^T, e_3^T)^T = (0^T, 0^T, 0^T)^T$, so we can also get that $f(e_1, e_3) \geq c_1 V^{\frac{\alpha+1}{2}}$. Similarly, define $g(e_1, e_3) = \|e_1\|_2^{\beta+1} + \|e_3\|_2^{\beta+1}$, then we can get $g(e_1, e_3) \geq c_3 V^{\frac{\beta+1}{2}}$, where $c_3 = \min g(V^{-\frac{1}{2}} e_1, V^{-\frac{1}{2}} e_3) > 0$.

Thus, the derivative of V (55) can be rewritten as follows

$$\dot{V} \leq -k_1 c_1 V^{\frac{\alpha+1}{2}} - k_3 m^{\frac{1-\beta}{2}} c_3 V^{\frac{\beta+1}{2}}, \quad (57)$$

where $k_1 > 0, k_3 > 0, 0 < \alpha < 1, \beta > 0$.

By Lemma 2.2, V will reach zero in fixed-time, and the setting time is bounded and given by

$$T = \frac{2}{k_1 c_1 (1 - \alpha)} + \frac{2}{k_3 m^{\frac{1-\beta}{2}} c_3 (\beta - 1)}.$$

which implies that $e_1(t) \rightarrow \mathbf{0}$, $\bar{e}_2(t) \rightarrow \mathbf{0}$ and $e_3(t) \rightarrow \mathbf{0}$ in fixed-time T . Then, from Remark 3 we can easily get that $\lim_{t \rightarrow T} e_1 = \mathbf{0}$, $\lim_{t \rightarrow T} \bar{e}_2 = \mathbf{0}$ and $\lim_{t \rightarrow T} e_3 = \mathbf{0}$. Thus, $z_{1j} = z_{10}$, $z_{2j} = z_{20}$ and $z_{3j} = z_{30}$ for any $t \geq T$.

The proof is completed. \blacksquare

Remark 6: Comparing with the existing works on finite-time control (Du et al., 2017, 2015; Zhao et al., 2014; Zhao, Duan, Wen, & Zhang, 2013), from (49) in this paper the upper bound of the system convergence time for fixed-time control does not depend on the initial states of the system while only depends on system perimeters and control gains. From (49), we can see that if the control gains k_1 and k_3 is larger then the upper bound T of the system convergence time is smaller.

Remark 7: Denoted that $f(e_1, e_3) = \|e_1\|_2^{\alpha+1} + \|e_3\|_2^{\alpha+1}$, when $f(e_1, e_3) = 0$, i.e. $e_1 = \mathbf{0}$ and $e_3 = \mathbf{0}$ under distributed controllers (35) and (36), it can be obtained that $\bar{e}_2 = \mathbf{0}$.

Proof: When $e_1 = \mathbf{0}$ and $e_3 = \mathbf{0}$, according to Equation (20), we have $\tilde{z}_1 = \mathbf{0}$. From Equation (34), we can get $\dot{\tilde{e}}_2 = \mathbf{0}$. From Equations (32) and (48), we can obtain $\dot{e}_3 = \mathbf{0}$. Then according to (51), we can have $\dot{V} = 0$. The second-order derivative of Lyapunov function candidate V is

$$\begin{aligned}\ddot{V} &= \dot{e}_1^T \dot{e}_1 + e_1^T \ddot{e}_1 + \dot{e}_2^T \dot{e}_2 + \dot{e}_2^T \ddot{e}_2 + \dot{e}_3^T \dot{e}_3 + e_3^T \ddot{e}_3 \\ &= \dot{e}_1^T \dot{e}_1 + \dot{e}_2^T \ddot{e}_2.\end{aligned}\quad (58)$$

From Equation (34), we can get the second-order derivative of \tilde{e}_2 is

$$\begin{aligned}\ddot{\tilde{e}}_2 &= \dot{u}_{10} e_3 + u_{10} \dot{e}_3 - \mathcal{M} \text{diag}(\dot{u}_2) \tilde{z}_1 - \mathcal{M} \text{diag}(u_2) \dot{\tilde{z}}_1 \\ &= -\mathcal{M} \text{diag}(u_2) \dot{\tilde{z}}_1.\end{aligned}\quad (59)$$

Substituting (30) and (59) into (58), we get

$$\begin{aligned}\ddot{V} &= \dot{e}_1^T \dot{e}_1 - \dot{e}_1^T (\mathcal{M}^T)^{-1} \text{diag}(u_2) \mathcal{M}^T \tilde{e}_2 \\ &= \dot{e}_1^T [-k_1 \text{sig}(e_1)^\alpha - k_3 \text{sig}(e_1)^\beta] = 0.\end{aligned}\quad (60)$$

Using the definition of second-order derivative, we have

$$\begin{aligned}\ddot{V}(t) &= \lim_{\Delta t \rightarrow 0} \frac{\dot{V}(t + \Delta t) - \dot{V}(t)}{\Delta t} \\ &= \lim_{\Delta t \rightarrow 0} \frac{\dot{V}(t + \Delta t)}{\Delta t} \\ &= \lim_{\Delta t \rightarrow 0} \frac{V(t + \Delta t) - V(t)}{\Delta t^2} \\ &= \lim_{\Delta t \rightarrow 0} \frac{(e_1(t) + \Delta t \dot{e}_1(t))^T (e_1(t) + \Delta t \dot{e}_1(t))}{2\Delta t^2} \\ &= \lim_{\Delta t \rightarrow 0} \frac{\Delta t^2 \dot{e}_1^T(t) \dot{e}_1(t)}{2\Delta t^2} \\ &= \frac{1}{2} \dot{e}_1^T(t) \dot{e}_1(t).\end{aligned}\quad (61)$$

Then we can get $\dot{e}_1 = \mathbf{0}$. From Equations (30) and (47), we can get $\tilde{e}_2 = \mathbf{0}$. The proof is completed. ■

Remark 8: From the Theorem 1, our control objectives (13)–(15) are held in fixed-time T under the distributed controllers (35) and (36). Thus, from Lemma 3, the m mobile robots can converge to the formation pattern \mathcal{F} in fixed-time T , and it does not depend on the initial states of the system.

4. Simulation result

In this section, a simulation example is shown to demonstrate the validity of the designed fixed-time control algorithm. We consider a multiple mobile robots system under a directed communication graph as shown in Figure 2, which contains six followers F_1 – F_6 and a virtual leader L .

Figure 3 shows the desired position relationship between the followers F_1 – F_6 and the virtual leader L . The orthogonal coordinates of followers are chosen as $(p_{1x}, p_{1y}) = (2, 0)$, $(p_{2x}, p_{2y}) = (1, \sqrt{3})$, $(p_{3x}, p_{3y}) = (-1, \sqrt{3})$, $(p_{4x}, p_{4y}) = (-2, 0)$, $(p_{5x}, p_{5y}) = (-1, -\sqrt{3})$, and $(p_{6x}, p_{6y}) = (1, -\sqrt{3})$.

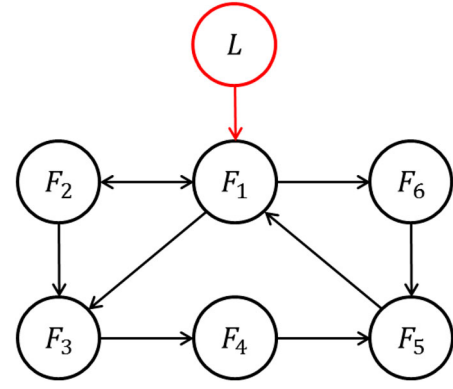


Figure 2. Directed communication graph among wheeled mobile robots.

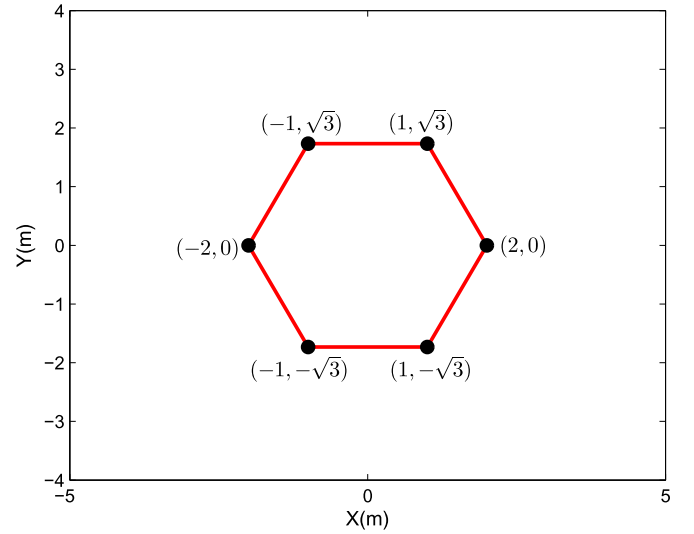


Figure 3. Desired geometric pattern of formation.

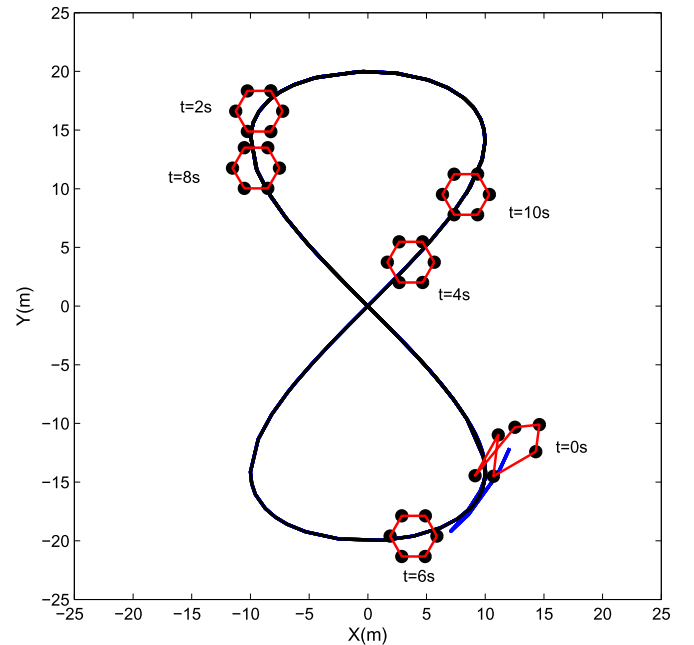


Figure 4. Formation pattern of the six follower robots at some time, the trajectory of virtual leader (black line) and the trajectory of centroid of the six follower robots (blue line) (Colour online).

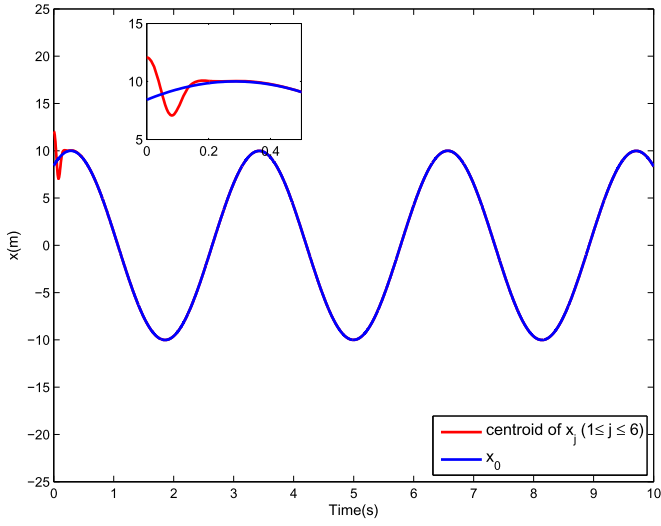


Figure 5. The trajectories of x_0 and the centroid of $x_j (1 \leq j \leq 6)$.

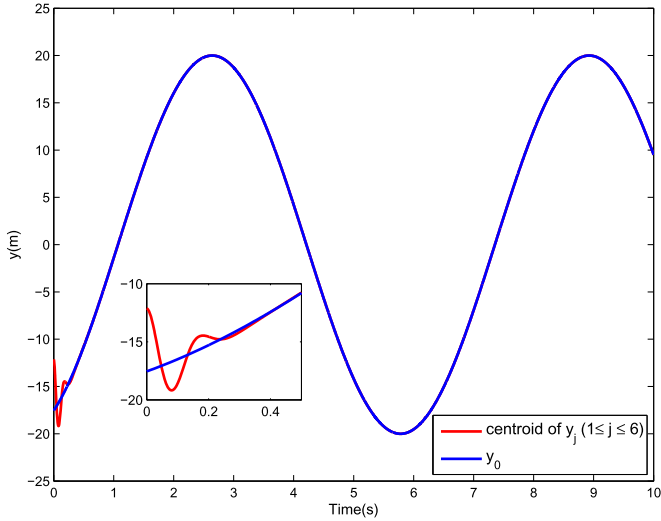


Figure 6. The trajectories of y_0 and the centroid of $y_j (1 \leq j \leq 6)$.

Define the virtual leader's trajectory, i.e. the reference trajectory as follows

$$x_0 = 10 \sin(2t + 1), \quad y_0 = -20 \cos(t + 1/2). \quad (62)$$

From Equation (62), we can get the virtual leader's linear velocity and angular velocity as follows

$$v_0 = 20 \sqrt{\sin(t + 1/2)^2 + \cos(2t + 1)^2}, \quad (63)$$

$$w_0 = \frac{2 \sin(t + 1/2) \sin(2t + 1) + \cos(t + 1/2) \cos(2t + 1)}{\sin(t + 1/2)^2 + \cos(2t + 1)^2}. \quad (64)$$

Accordint to the Theorem 3.2, the parameters of the simulation for the group of wheeled mobile robots are chosen as $k_1 = 10$, $k_2 = 1$, $k_3 = 5$, $\alpha = 0.9$, and $\beta = 1.1$.

As we can see from Figure 4, six wheeled mobile robots form the desired formation pattern under the distributed fixed-time controllers (35) and (36) with directed interaction topology. From Figures 5 and 6, the trajectory of the formation centre

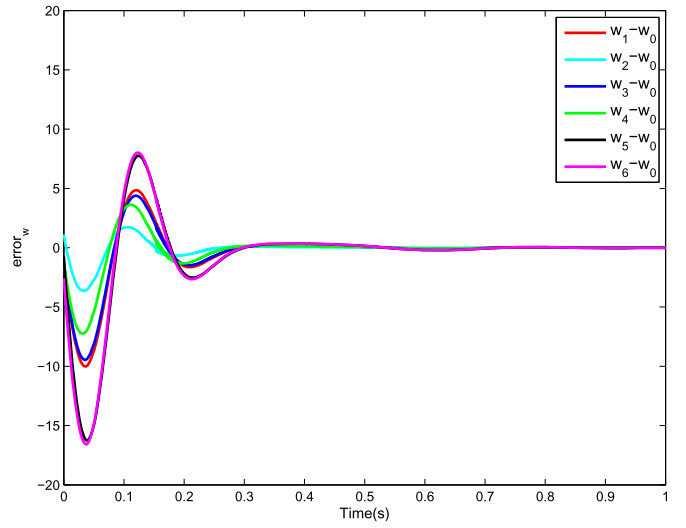


Figure 7. The tracking errors between $\omega_j (1 \leq j \leq 6)$ and ω_0 .

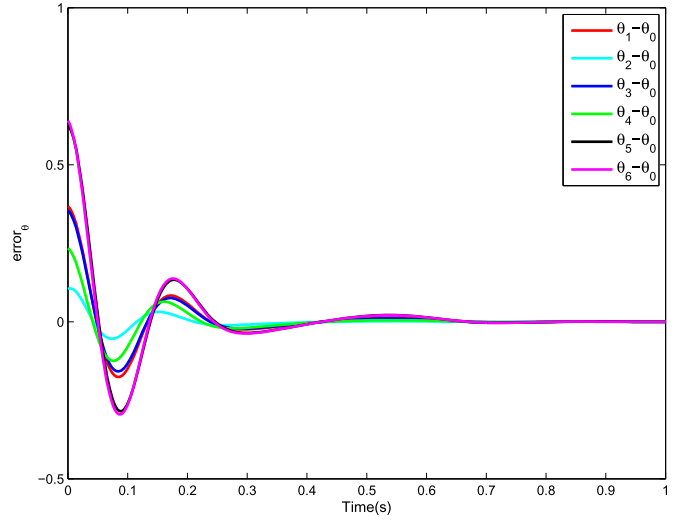


Figure 8. The tracking errors between $\theta_j (1 \leq j \leq 6)$ and θ_0 .

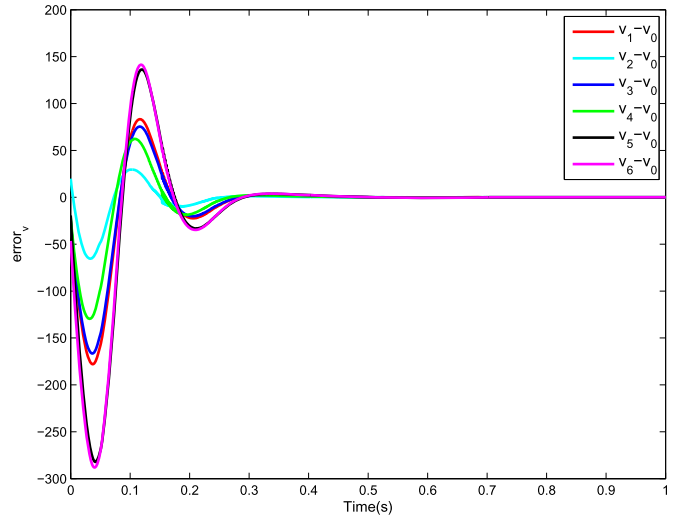


Figure 9. The tracking errors between $v_j (1 \leq j \leq 6)$ and v_0 .

of the six robots can successfully track the trajectory of the virtual leader in 0.4 s. From Figures 7, 8 and 9, we can see that the angular velocity, orientation and linear velocity of the robot j are reached the virtual leader's, respectively. Therefore, we can say that the control objectives (6)–(8) are achieved under the distributed fixed-time controllers (35) and (36) with directed interaction topology.

If the control gain $k_3 = 0$, the controllers (35) and (36) become the finite-time controllers. Simulation shows that the larger the control gain k_3 , the faster the convergence speed and the smaller the amplitude of the errors.

5. Conclusion

In this paper, the distributed fixed-time controllers are proposed to deal with the formation tracking control problem of multiple wheeled mobile robots under directed topology. Utilizing the graph theory and Lyapunov stability theory, the stability of formation control is verified. In addition, the effectiveness of the proposed fixed-time controllers are verified by numerical simulation. In this paper, the communication between the robots is continuous and the states in the controllers are continuously updated, which causes the waste of resources. Therefore, in the subsequent study we will consider using event-triggered to reduce the communication between robots and the number of states update. In addition, considering the state and input information may be not available in practice Du et al. (2015), some kinds of observers need to be designed. Hence, observer-based fixed-time control will also be a future research direction.

Disclosure statement

No potential conflict of interest was reported by the authors.

Funding

This work was supported by the National Natural Science Foundation of China [grant number 61503016], and the National Key R&D Program of China [grant numbers 2017YFB0103202 and 2016YFB0100307], and the Fundamental Research Funds for the Central Universities [grant numbers YWF-19-BJ-J-259, YWF-18-BJ-J-229, YWF-15-SYS-JTXY-007, YWF-16-BJ-Y-21 and 2017JBM067].

ORCID

Guoquan Wen  <http://orcid.org/0000-0001-9128-1802>

References

- Balch, T., & Arkin, R. C. (1998). Behavior-based formation control for multirobot teams. *IEEE Transactions on Robotics and Automation*, 14, 926–939.
- Cheng, L., Wang, Y., Ren, W., Hou, Z. G., & Tan, M. (2016). Containment control of multiagent systems with dynamic leaders based on a PI^n -type approach. *IEEE Transactions on Cybernetics*, 46, 3004–3017.
- Chu, X., Peng, Z., Wen, G., & Rahmani, A. (2017). Decentralised consensus-based formation tracking of multiple differential drive robots. *International Journal of Control*, 90, 2461–2470.
- Chu, X., Peng, Z., Wen, G., & Rahmani, A. (2018). Robust fixed-time consensus tracking with application to formation control of unicycles. *IET Control Theory Applications*, 12, 53–59.
- Das, A. K., Fierro, R., Kumar, V., Ostrowski, J. P., Spletzer, J., & Taylor, C. J. (2002). A vision-based formation control framework. *IEEE Transactions on Robotics and Automation*, 18, 813–825.
- Dong, X., Yu, B., Shi, Z., & Zhong, Y. (2015). Time-varying formation control for unmanned aerial vehicles: Theories and applications. *IEEE Transactions on Control Systems Technology*, 23, 340–348.
- Du, H., Jiang, C., Wen, G., Zhu, W., & Cheng, Y. (2018). Current sharing control for parallel dc-dc buck converters based on finite-time control technique. *IEEE Transactions on Industrial Informatics*. Advance online publication. doi:10.1109/TII.2018.2864783
- Du, H., Wen, G., Cheng, Y., He, Y., & Jia, R. (2017). Distributed finite-time cooperative control of multiple high-order nonholonomic mobile robots. *IEEE Transactions on Neural Networks and Learning Systems*, 28, 2998–3006.
- Du, H., Wen, G., Yu, X., Li, S., & Chen, M. Z. (2015). Finite-time consensus of multiple nonholonomic chained-form systems based on recursive distributed observer. *Automatica*, 62, 236–242.
- Du, H., Zhu, W., Wen, G., Duan, Z., & Lü, J. (2019). Distributed formation control of multiple quadrotor aircraft based on nonsmooth consensus algorithms. *IEEE Transactions on Cybernetics*, 49(1), 342–353.
- Hong, H., Yu, W., Wen, G., & Yu, X. (2016). *Distributed robust fixed-time consensus in multi-agent systems with nonlinear dynamics and uncertain disturbances*. 2016 IEEE international conference on industrial technology (ICIT), Taipei, Taiwan, 14–17 March 2016. 1390–1395.
- Hu, X. (2001). Formation constrained multi-agent control. *IEEE Transactions on Robotics and Automation*, 17, 947–951.
- Hu, J., & Feng, G. (2010). Distributed tracking control of leader-follower multi-agent systems under noisy measurement. *Automatica*, 46, 1382–1387.
- Lawton, J. R. T., Beard, R. W., & Young, B. J. (2003). A decentralized approach to formation maneuvers. *IEEE Transactions on Robotics and Automation*, 19, 933–941.
- Lewis, M. A., & Tan, K.-H. (1997). High precision formation control of mobile robots using virtual structures. *Autonomous Robots*, 4, 387–403.
- Murray, R. M., & Sastry, S. S. (1993). Nonholonomic motion planning: Steering using sinusoids. *IEEE Transactions on Automatic Control*, 38, 700–716.
- Ni, J., Liu, L., Liu, C., & Hu, X. (2017). Fractional order fixed-time nonsingular terminal sliding mode synchronization and control of fractional order chaotic systems. *Nonlinear Dynamics*, 89, 2065–2083.
- Olfati-Saber, R. (2005). Ultrafast consensus in small-world networks. In *Proceedings of the 2005, American Control Conference*, (Vol. 5, pp. 2371–2378).
- Olfati-Saber, R., & Murray, R. M. (2004). Consensus problems in networks of agents with switching topology and time-delays. *IEEE Transactions on Automatic Control*, 49, 1520–1533.
- Peng, Z., Wen, G., Rahmani, A., & Yu, Y. (2013). Leader-follower formation control of nonholonomic mobile robots based on a bioinspired neurodynamic based approach. *Robotics and Autonomous Systems*, 61, 988–996.
- Peng, Z., Wen, G., Yang, S., & Rahmani, A. (2016). Distributed consensus-based formation control for nonholonomic wheeled mobile robots using adaptive neural network. *Nonlinear Dynamics*, 86, 605–622.
- Polyakov, A. (2012). Nonlinear feedback design for fixed-time stabilization of linear control systems. *IEEE Transactions on Automatic Control*, 57, 2106–2110.
- Sarkar, S., & Kar, I. N. (2016). Formation of multiple groups of mobile robots: multi-timescale convergence perspective. *Nonlinear Dynamics*, 85, 2611–2627.
- Shojaei, K. (2017). Output-feedback formation control of wheeled mobile robots with actuators saturation compensation. *Nonlinear Dynamics*, 89, 2867–2878.
- Wang, J. L., Wu, H. N., Huang, T., Ren, S. Y., & Wu, J. (2017). Passivity analysis of coupled reaction-diffusion neural networks with dirichlet boundary conditions. *IEEE Transactions on Systems, Man, and Cybernetics: Systems*, 47, 2148–2159.
- Wen, G., Yu, Y., Peng, Z., & Rahmani, A. (2016). Distributed finite-time consensus tracking for nonlinear multi-agent systems with a time-varying reference state. *International Journal of Systems Science*, 47, 1856–1867.
- Wenjie, D. (2011). Flocking of multiple mobile robots based on backstepping. *IEEE Transactions on Systems, Man, and Cybernetics, Part B: Cybernetics*, 41, 414–424.

- Xiao, B., Hu, Q., & Zhang, Y. (2015). Finite-time attitude tracking of spacecraft with fault-tolerant capability. *IEEE Transactions on Control Systems Technology*, 23, 1338–1350.
- Zhang, B., & Jia, Y. (2015). Fixed-time consensus protocols for multi-agent systems with linear and nonlinear state measurements. *Nonlinear Dynamics*, 82, 1683–1690.
- Zhao, Y., Duan, Z., & Wen, G. (2014). Finite-time consensus for second-order multi-agent systems with saturated control protocols. *IET Control Theory and Applications*, 9, 312–319.
- Zhao, Y., Duan, Z., Wen, G., & Zhang, Y. (2013). Distributed finite-time tracking control for multi-agent systems: An observer-based approach. *Systems & Control Letters*, 62, 22–28.
- Zuo, Z., & Tie, L. (2016). Distributed robust finite-time nonlinear consensus protocols for multi-agent systems. *International Journal of Systems Science*, 47, 1366–1375.